

VRDMG: VOCAL RESTORATION VIA DIFFUSION POSTERIOR SAMPLING WITH MULTIPLE GUIDANCE

Carlos Hernandez-Olivan^{1,*} Koichi Saito² Naoki Murata² Chieh-Hsin Lai²
Marco A. Martínez-Ramírez² Wei-Hsiang Liao² Yuki Mitsufuji^{2,3}

¹Dept. of Electronic Engineering and Communications, University of Zaragoza, Spain

²Sony AI, Tokyo, Japan

³Sony Group Corporation, Tokyo, Japan

ABSTRACT

Restoring degraded music signals is essential to enhance audio quality for downstream music manipulation. Recent diffusion-based music restoration methods have demonstrated impressive performance, and among them, diffusion posterior sampling (DPS) stands out given its intrinsic properties, making it versatile across various restoration tasks. In this paper, we identify that there are potential issues which will degrade current DPS-based methods' performance and introduce the way to mitigate the issues inspired by diverse diffusion guidance techniques including the Re-Paint (RP) strategy and the Pseudoinverse-Guided Diffusion Models (IIGDM). We demonstrate our methods for the vocal declipping and bandwidth extension tasks under various levels of distortion and cutoff frequency, respectively. In both tasks, our methods outperform the current DPS-based music restoration benchmarks. We refer to <http://carlosholivan.github.io/demos/audio-restoration-2023.html> for examples of the restored audio samples.

Index Terms— Inverse problems, voice restoration, diffusion model, deep learning, diffusion posterior sampling

1. INTRODUCTION

Music restoration is framed as an inverse problem with the objective of recovering a degraded music signal. In this domain, the tasks such as inpainting, declipping, bandwidth extension, and dereverberation are prevalent [1]. These tasks are ill-posed, indicating that multiple restoration outcomes could be equally valid. Various techniques have been proposed to address these issues, ranging from unsupervised methods based on signal processing to supervised deep neural network (DNN) approaches using paired degraded and clean signals [2–5]. These methods may not operate robustly when the target audio deviates from the underlying assumptions or the characteristics of the paired data used for training. Additionally, we need to prepare assumptions and paired data for each task.

On the other hand, recent approaches utilize deep generative models trained solely on clean signals as a prior to retrieve the clean signal from observed data [1, 6–10]. This paradigm does not require degraded signals during training, allowing for a data-driven acquisition of assumptions solely about the clean signals. It offers the advantage of being adaptable to various tasks without the need for retraining. Among these, notably, unsupervised diffusion-based approaches have demonstrated significant performance [6–8, 10].

CQT-Diff [7] addresses challenges in piano declipping, bandwidth extension, and inpainting by employing diffusion posterior sampling (DPS) [11] in conjunction with the reconstruction guidance (RG) [12] and the data consistency (DC) method [13]. While the method demonstrates impressive performance, there remains room for improvement in several aspects. Expanding from RG, the Pseudoinverse-Guided Diffusion Models (IIGDM) [14] have been introduced to address inverse problems not only rooted in noisy and non-linear degraded measurements but also when confronted with a non-differentiable degradation function. Moreover, empirical evaluations by the authors reveal IIGDM outperform DPS with even fewer diffusion steps, indicative of its computational efficiency. Although the DC method has been recognized for its proficient performance, it is not without its limitations. RePaint (RP) [15] highlighted that the application of the DC method for image inpainting results in the predicted region mirroring the texture of the adjacent regions, yet being semantically inconsistent. The implications of semantic inaccuracy introduced by the DC method potentially degrading performance in music restoration tasks. Furthermore, while the empirical validation of CQT-Diff has been confined to piano data, its efficacy on datasets with diverse distributions, such as vocal data [16], remains unexplored.

In this paper, we enhance DPS-based music restoration and evaluate its efficacy on diverse vocal data. Our contribution can be summarized as five parts. We introduce the RP strategy [15] with time scheduling inspired by FreeDoM [17]. Additionally, we refine RG by incorporating time-dependent scaling and the IIGDM method. Given the inherent orthogonality of these approaches, we conduct comprehensive experiments on declipping and bandwidth extension task and ascertain the most effective combination. Comparing inference speeds between the CQT-Diff (CQT model) and SaShiMi-Diff (1D model) architectures from [7], by applying our techniques, we find the 1D model achieves comparable performance to the CQT model but boasts an 15x faster inference time.

2. RELATED WORK

Prior to the application of diffusion models to audio restoration, problem-specific models were introduced for challenges like declipping [2, 3] and bandwidth extension [5, 18]. Following the success of unsupervised diffusion-based approaches in image domain, there has been a growing interest in problem-agnostic frameworks [10, 11, 14, 19]. Music restoration spans various challenges, all potentially benefiting from unified approaches adept at addressing these distinct tasks via posterior sampling. Several unsupervised diffusion-

*This work has been done during an internship at Sony

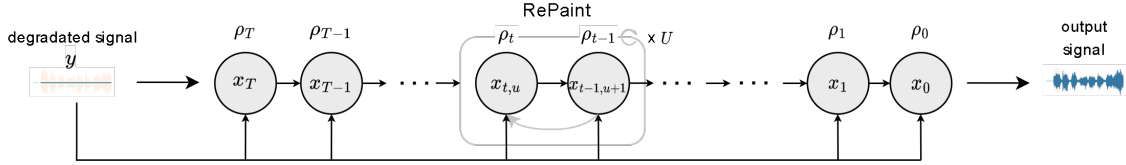


Fig. 1. Inference process of our RG $\delta\rho$ + DC + RP method. ρ_t is the parameter that controls the gradients weighting and \mathbf{x}_t is the prediction at each diffusion step t . U are the repainting steps.

based methods with this aim have emerged, focusing on piano data [7] or vocal data [8]. CQT-Diff [7] offers a unified strategy for piano restoration, effectively recovering piano signals for a range of tasks and their specific degradations: inpainting, bandwidth extension, and declipping.

To the best of our knowledge, DPS [11] and its variants, which have found applications in image domain [14, 15, 17], remain inadequately explored for audio restoration tasks. In this study, we showcase the potential enhancements achievable by transitioning techniques from image domain, such as IIGDM [14] and RePaint [15], to the realm of audio domain, thereby amplifying the efficacy of RG and DC.

3. VOCAL RESTORATION VIA DIFFUSION POSTERIOR SAMPLING

3.1. Score-based Generative Modeling

Let us denote the data distribution of clean signals by p_{data} . Consider a diffusion process wherein a clean signal $\mathbf{x}_0 \sim p_{\text{data}}$ is progressively diffused into an intermediate noisy signal \mathbf{x}_t over time step $t = 0, \dots, T$ with associated noise levels $\sigma_T = \sigma_{\text{max}} > \dots > \sigma_t > \sigma_{t-1} > \dots > \sigma_0 = \sigma_{\text{min}}$. The terminal point \mathbf{x}_T is characterized as Gaussian noise $\mathbf{x}_T \sim \mathcal{N}(0, \sigma_{\text{max}}^2 \mathbf{I})$.

Diffusion models [20–22], alternatively termed score-based models, generate a clean signal through the reverse diffusion process. These models approximate the gradient of the logarithmic probability density relative to the score function $\nabla_{\mathbf{x}_t} \log p_t(\mathbf{x}_t)$ [23]. The reverse diffusion process can be articulated by the following Stochastic Differential Equation (SDE) [22]:

$$d\mathbf{x}_t = \left(\frac{1}{2}g(t)^2 - \dot{\sigma}(t)\sigma(t) \right) \nabla_{\mathbf{x}_t} \log p_t(\mathbf{x}_t) dt + g(t) d\mathbf{w}_t \quad (1)$$

where w denotes the standard Wiener process, $\dot{\sigma}(t)$ represents the time derivative of noise levels at time t , and $g(t)$ is *diffusion* coefficient of \mathbf{x}_t [24].

In the diffusion models, the score function is approximated utilizing a neural network $D_{\theta}(\mathbf{x}; \sigma)$, where θ are the parameters of neural network. In EDM [22], upon which our work is predicated, the score function is estimated as $\nabla_{\mathbf{x}_t} \log p_t(\mathbf{x}_t; \sigma_t) = (D_{\theta}(\mathbf{x}_t; \sigma_t) - \mathbf{x}_t) / \sigma_t^2$, where the neural network of the denoiser $D_{\theta}(\mathbf{x}_t; \sigma_t)$ is trained with the following L_2 objective:

$$\mathbb{E}_{\mathbf{x}_{\text{data}} \sim p_{\text{data}}, \mathbf{n} \sim \mathcal{N}(0, \sigma_t^2 \mathbf{I})} [\|D_{\theta}(\mathbf{x}_{\text{data}} + \mathbf{n}; \sigma_t) - \mathbf{x}_{\text{data}}\|_2^2], \quad (2)$$

where $\mathbf{x}_{\text{data}} \sim p_{\text{data}}$ is a training data. By solving the SDE by substituting the estimated score function with discrete sampling times t , the models can generate samples.

3.2. Inverse Problem via Posterior Sampling

The objective of music inverse problem is to recover the clean music signal \mathbf{x}_0 from observed degraded signal $\mathbf{y} = \mathcal{A}(\mathbf{x}_0) + \epsilon$, where $\mathcal{A}(\cdot)$ represents the degradation function, $\epsilon \sim \mathcal{N}(0, \sigma_y^2 \mathbf{I})$ is the measurement noise and σ_y^2 is

noise variance of measurement. To address inverse problems through diffusion models, we can substitute the score $\nabla_{\mathbf{x}_t} \log p_t(\mathbf{x}_t)$ in Eq. 1 for the conditional score function $\nabla_{\mathbf{x}_t} \log p_t(\mathbf{x}_t | \mathbf{y})$ [7, 11]. Within the Bayesian framework, the *posterior* $p(\mathbf{x} | \mathbf{y})$ can be expressed as $p(\mathbf{x} | \mathbf{y}) \propto p(\mathbf{x})p(\mathbf{y} | \mathbf{x})$. Leveraging this relationship, the conditional score $\nabla_{\mathbf{x}_t} \log p_t(\mathbf{x}_t | \mathbf{y})$ can be deduced as:

$$\nabla_{\mathbf{x}_t} \log p_t(\mathbf{x}_t | \mathbf{y}) = \nabla_{\mathbf{x}_t} \log p_t(\mathbf{x}_t) + \nabla_{\mathbf{x}_t} \log p_t(\mathbf{y} | \mathbf{x}_t). \quad (3)$$

In Eq. (3), it's essential to evaluate two components; the first term is the score function which we can compute via $(D_{\theta}(\mathbf{x}_t; \sigma_t) - \mathbf{x}_t) / \sigma_t^2$ and the second term is likelihood which can be computed as [11]:

$$\nabla_{\mathbf{x}_t} \log p_t(\mathbf{y} | \mathbf{x}_t) \simeq -\rho(t) \nabla_{\mathbf{x}_t} \|\mathbf{y} - \mathcal{A}(D_{\theta}(\mathbf{x}_t; \sigma_t))\|^2. \quad (4)$$

We refer to this method reconstruction guidance (RG) [7, 12].

The gradient in Eq. 4 is scaled by a time-dependent scaling function $\rho(t)$. In CQT-Diff [7], $\rho(t)$ is empirically determined so that $\rho(t) = \rho' \sqrt{L} / (t \|G\|^2)$, where $G = \nabla_{\mathbf{x}_t} \|\mathbf{y} - \mathcal{A}(D_{\theta}(\mathbf{x}_t; \sigma_t))\|^2$, where L is the sample length of audio signal and ρ' is a constant value. In our work, drawing inspiration from the segmented stages of diffusion sampling as depicted in [17, Fig.3], we empirically find that redefining $\rho(t)$ as $\rho(t)\delta\rho$, where $\delta\rho = (T - t)/75$ exhibits superior performance compared to a static ρ' . Defining $\delta\rho$ in this manner, the scale of RG remains small during the initial stages of the diffusion process (or the chaotic phase) where the generation is out of control according to FreeDoM [17]. As the diffusion process progresses and the generation becomes more controllable, the scale of RG becomes large.

3.3. Pseudo-Inverse Guidance

The second term of Eq. (4) can alternatively be calculated by utilizing Pseudo-inverse Guidance (IIGDM) [14] as:

$$\nabla_{\mathbf{x}_t} \log p_t(\mathbf{y} | \mathbf{x}_t) \simeq \left((h^{\dagger}(\mathbf{y}) - h^{\dagger}(h(\hat{\mathbf{x}}_0)))^{\top} \frac{\partial \hat{\mathbf{x}}_0}{\partial \mathbf{x}_t} \right)^{\top}, \quad (5)$$

where $\hat{\mathbf{x}}_0$ is estimated clean signal by the denoiser network $D_{\theta}(\mathbf{x}_t; \sigma_t)$, h is a non-linear degradation function, and h^{\dagger} need to adhere to the equation $h(h^{\dagger}(h(\mathbf{x}))) = h(\mathbf{x})$ for all \mathbf{x} . h and h^{\dagger} can be even non-differentiable degradation function, rendering DPS inapplicable. Empirical evaluations by the authors [14] reveal IIGDM outperform RG with even fewer diffusion steps, indicative of its computational efficiency.

3.4. Improving Data Consistency method

In previous study [7], the DC method is applied during sampling. The DC method substitutes the intermediate prediction $\hat{\mathbf{x}}_0 = D_{\theta}(\mathbf{x}_t; \sigma_t)$ with the measurement \mathbf{y} every discrete sampling step. On the image inpainting task, RePaint [15] points out that only applying the DC method leads that the predicted region only matches the texture of the adjacent regions, thereby being semantically inaccurate. This phenomenon can potentially be observed in inverse problem

utilizing the DC method on music domain, leading to worse restoration performance.

To alleviate this limitation, we advocate integrating the RePaint (RP) strategy [15] with the DC method. The RP strategy is a resampling strategy that first diffuses output \mathbf{x}_{t-1} back to \mathbf{x}_t through the sampling as:

$$\mathbf{x}_t \sim \mathcal{N}(\mathbf{x}_{t-1}, (\sigma_t^2 - \sigma_{t-1}^2)\mathbf{I}) \quad (6)$$

and then conducts regular reverse diffusion step from \mathbf{x}_t , again. We designate this one cycle as the RP cycle. Originally, the RP strategy is applied with every diffusion step during inference with multiple the RP cycle (Please refer to [15, Algo. 1]). Even in the absence of the RP strategy, diffusion models generally need multiple sampling steps to generate samples, which is time consuming. Hence, applying multiple RP cycles will result in an increased number of sampling steps. To circumvent this issue, we propose to apply the RP cycle exclusively during the phase which crucially affects sampling outcome inspired by the categorized stages of diffusion sampling [17, Fig.3]. We define the number of the RP cycles U depending on the entire number of the diffusion steps T as:

$$U = \begin{cases} 0 & \forall t < \phi_1 T/3 \\ u & \forall \phi_1 T/3 \leq t \leq \phi_2 T/3 \\ 0 & \forall t > \phi_2 T/3 \end{cases} \quad (7)$$

where ϕ_1 and ϕ_2 are term to define when the RP cycle starts and end in inspired by FreeDoM [17].

4. EXPERIMENTS AND RESULTS

4.1. Dataset

To evaluate the methods under the various types of vocals, we use vocal data which do not contain audio effects (dry vocals) and contain audio effects (wet vocals). For pre-training of diffusion models, we use the NHSS dataset [25], which only contains dry vocals, and an internal dataset of wet vocals. The NHSS dataset contains 100 English pop songs (20 unique songs) of ten different male and female singers. The total duration of the dataset is 95.76h for training and 0.94h for validation. For evaluation, we use the NUS dataset [26], which contains dry vocals, and the wet vocals from MUSDB18 dataset [27]. We downsample all the tracks to 22.05 kHz. Due to the time constraints, We selected 200 random segments of 2.97 seconds for both dry and wet vocals, ensuring that they encompassed a diverse range of vocalists.

4.2. Model Configurations

In our preliminary experiments, we observe that the CQT-Diff (CQT model) requires more time to output restored data compared to the SaShiMi-Diff (1D model), due to its inverse CQT implementation [7, 28]. Both models are referred in [7, Section 3.1]. Consequently, we train those two types of models and evaluate both in terms of performance and inference time. The difference between these two models is the input data representation for the neural network. In the 1D model, the neural network receives input in the form of a waveform representation. On the other hand, in the CQT model, the input data representation is CQT representation.

Both models have a U-Net architecture comprising the six layers with the dilated convolutions and the GELU activations. Both models have 15M parameters. We use Adam optimizer and an initial learning rate of $2e - 4$. The noise

variance schedule at diffusion step t , σ_t , follows the expression:

$$\sigma_t = \left(\sigma_{\max}^{\frac{1}{\nu}} + \frac{t}{T-1} \left(\sigma_{\min}^{\frac{1}{\nu}} - \sigma_{\max}^{\frac{1}{\nu}} \right) \right)^{\nu} \quad t = T \dots 1 \quad (8)$$

We set $\nu = 13$, $\sigma_{\min} = 10^{-4}$, $\sigma_{\max} = 1$ and $S_{\text{churn}} = 5$ for the noise variance schedule [22]. For inference step, we utilize $T = 300$ diffusion steps.

4.3. Declipping

Declipping an audio signal is restoring the signal after a distortion with a threshold c has been applied to it. The degradation function is formulated as $\mathcal{A}(\mathbf{x}_0) = (|\mathbf{x}_0 + c| - |\mathbf{x}_0 - c|)/2$. This is hard-clipping setting [3]. We perform both objective and subjective evaluations. The objective evaluation is measured in terms of the Fréchet Audio Distance (FAD) [29] and the Scale-Invariant Signal-to-Distortion Ratio (SI-SDR) [30].

We test both models with the different sampling methods: RG and RG + DC as the baseline methods proposed in [7], and our proposed methods: RG $\delta\rho$ + DC, which consists on applying RG with DC method and $\delta\rho$, RG $\delta\rho$ + DC + RP and DC + IIGDM. With employing the RP strategy, Eq. 6 is invoked with $u = 10$, $\phi_1 = 1.5$ and $\phi_2 = 2.8$, leading to the $U = 10$ RP cycles between the diffusion steps $t = 150$ to $t = 20$. For the IIGDM method, we define $h(\mathbf{x}) = \mathcal{A}(\mathbf{x})$ and $h^\dagger(\mathbf{x}) = \mathcal{A}(\mathbf{x})$. With this definition, $h(h^\dagger(h(\mathbf{x}))) = h(\mathbf{x})$ is satisfied, as illustrated in Eq. 5. We compare the models and methods with two Signal-to-Distortion Ratio (SDR) of applied clipping, 5dB and 10dB as it is reported in Table 1.

In terms of the 1D model, RG $\delta\rho$ + DC + RP consistently outperforms all of the other methods for all the experimental settings. As for the CQT model, upon overall consideration, RG $\delta\rho$ + DC + RP tends to show better performance than the other methods. From these observations, combining all the method, which are $\delta\rho$, the DC method, and the RP strategy, is effective to enhance the performance of the original RG method. Moreover, comparing with RG $\delta\rho$ + DC + RP of the 1D and the CQT model, it is remarkable that the 1D model tends to show better scores since the inference time of the 1D model is $\times 15$ faster than the CQT model using the a RTX 3090 24Gb GPU. The actual inference time of the 1D model using RG $\delta\rho$ + DC + RP is three minutes and the CQT model takes 45 minutes.

We also conducted a listening test using the multiple stimuli with the hidden reference and anchor (MUSHRA) protocol [31]. We ask the 12 participants to rate the quality of the restored signals with the different methods. To avoid the listening fatigue, we only include the samples from the CQT models under SDR = 5dB, which is harsher setting as the objective evaluation proves. Also, we discarded the worst-performing methods (RG) and (RG + DC) according to the objective results in Table 1. The results of the listening test are illustrated in Fig 2. In both dry and wet configurations, RG $\delta\rho$ + DC + RP show the best score as we see in Table 1. Notably, within the wet setting, RG $\delta\rho$ + DC + RP is perceived by the listeners to be very close to the reference.

4.4. Bandwidth Extension

Bandwidth extension consists on restoring the frequencies that have been removed from the signal with a low pass filter (LPF). Within this configuration, the degradation function of bandwidth extension is formulated as $\mathcal{A}(\mathbf{x}) = \text{LPF}(\mathbf{x})$. We evaluate the methods with two settings of cutoff frequencies $f_c = 3$ and 5 kHz. For the IIGDM method, same

Table 1. Objective metrics for declipping with pre-trained CQT and 1D models. For each metric and test set, each result is highlighted in bold and second best result is underlined.

	Method	SDR = 5dB				SDR = 10dB			
		FAD		SI-SDR		FAD		SI-SDR	
		↓ dry	↓ wet	↑ dry	↑ wet	↓ dry	↓ wet	↑ dry	↑ wet
	Clipped	3.48	2.25	6.42	5.06	1.10	0.87	11.08	9.18
1D	RG [7]	1.84	1.55	9.79	5.36	0.66	1.19	14.39	7.76
	RG + DC	0.94	1.05	10.13	<u>6.15</u>	0.66	0.52	14.48	<u>8.69</u>
	RG $\delta\rho$ + DC	0.88	1.00	10.97	6.03	<u>0.35</u>	<u>0.32</u>	14.79	8.57
	IIGDM + DC	2.76	1.73	5.44	3.18	1.02	0.76	10.31	7.01
	RG $\delta\rho$ + DC + RP	0.47	0.65	11.83	7.03	0.15	0.21	15.42	9.05
CQT	RG [7]	1.59	1.05	9.87	5.76	0.37	1.04	14.29	8.20
	RG + DC	1.16	0.80	10.09	6.24	0.37	0.39	14.33	<u>8.91</u>
	RG $\delta\rho$ + DC	0.52	0.34	<u>10.58</u>	<u>6.51</u>	<u>0.16</u>	0.19	14.50	9.02
	IIGDM + DC	2.62	1.57	5.70	3.75	0.74	0.60	10.70	7.22
	RG $\delta\rho$ + DC + RP	<u>0.73</u>	1.02	11.61	7.33	0.13	<u>0.28</u>	15.03	8.75

Table 2. Objective metrics for bandwidth extension with pre-trained CQT and 1D models

Model	Method	$f_c = 3\text{KHz}$				$f_c = 5\text{KHz}$			
		FAD		LSD		FAD		LSD	
		↓ dry	↓ wet	↓ dry	↓ wet	↓ dry	↓ wet	↓ dry	↓ wet
	LPF	4.12	3.16	4.26	4.55	2.53	1.79	3.61	3.86
1D	RG [7]	2.38	1.35	1.87	1.95	1.72	1.00	1.59	1.86
	RG + DC [7]	1.53	1.44	<u>1.98</u>	1.84	<u>0.57</u>	0.44	<u>1.67</u>	<u>1.61</u>
	RG $\delta\rho$ + DC	1.13	1.38	2.01	1.89	0.46	<u>0.48</u>	1.57	<u>1.61</u>
	IIGDM + DC	1.69	1.26	2.14	<u>1.86</u>	0.67	<u>0.48</u>	1.93	1.70
	RG $\delta\rho$ + DC + RP	1.15	1.46	2.00	1.88	0.73	0.58	1.56	1.60
CQT	RG [7]	1.63	0.75	1.95	1.91	1.31	0.82	1.70	1.79
	RG + DC [7]	1.06	<u>0.65</u>	<u>2.01</u>	<u>1.82</u>	0.39	0.30	<u>1.67</u>	1.59
	RG $\delta\rho$ + DC	1.65	1.17	2.34	2.10	0.44	0.35	1.64	<u>1.61</u>
	IIGDM + DC	1.06	0.63	2.00	1.80	1.23	<u>0.32</u>	1.68	1.66
	RG $\delta\rho$ + DC + RP	1.78	1.57	2.31	2.03	0.51	0.67	1.68	1.62

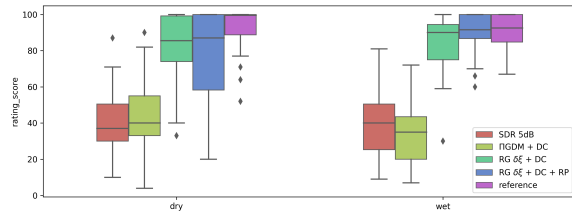


Fig. 2. Results of the audio declipping listening test of CQT model for 5dB.

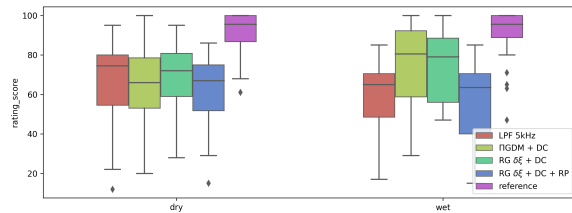


Fig. 3. Results of the audio bandwidth extension listening test of CQT model for 5kHz.

as the declipping setting, we define $h(\mathbf{x}) = \mathcal{A}(\mathbf{x})$ and $h^\dagger(\mathbf{x}) = \mathcal{A}(\mathbf{x})$. With this definition, if we assume that the LPF can cutoff all the frequency components lower than f_c , $h(h^\dagger(h(\mathbf{x}))) = h(\mathbf{x})$ is satisfied, as illustrated in Eq. 5 since applying consecutive the LPF with the same f_c to the signal is the same as applying it once. In this task, we set $\phi_1 = 2.5$, $\phi_2 = 2.8$ and $u = 5$ for the RP strategy.

In this case, the objective evaluation shows that the best-performing methods are RG + DC and IIGDM + DC. In contrast with the declipping task, IIGDM performs well and outperforms other techniques like RG. Is also worth noticing that RP does not work that well in this task. The reason why

RP does not work for this task might be due to the diffusion trajectories that the time-traveling introduces itself which for bandwidth extension are not optimal.

In parallel to the declipping task, we conducted a listening test, engaging the same participants to evaluate the methods for the $f_c = 5$ kHz case. The results of the bandwidth extension listening test are presented in Fig. 3. The subjective evaluation reports that the best method for $f_c = 5$ kHz is RG $\delta\rho$ + DC. The listening test results show that any of the methods outperform the lowpassed signal for the dry vocals. The human auditory system is highly attuned to the formants of speech. Consequently, due to the absence of effects in dry signals containing only the voice, the inadequate reconstruction of these formants might be more perceptible to the human ear compared to wet signals where effects mask this imperfect formant reconstruction. In wet signals, we can observe how IIGDM and RG $\delta\rho$ + DC perform better, which also happens in the objective evaluation.

5. CONCLUSIONS

In this study, we analyzed various diffusion sampling techniques for music restoration. We pointed out potential shortcomings in the current DPS-based methods and introduced the way to address them. By incorporating the RP strategy, IIGDM, and time-dependent weights for the guidance term, we enhanced restoration performance in both vocal declipping and bandwidth extension tasks, outclassing the baseline methods. Notably, the 1D model, when using the same sampling technique, achieved equivalent performance to the CQT model but was 15 times faster.

6. REFERENCES

- [1] Vivek Sivaraman Narayanaswamy, Jayaraman J. Thiagarajan, and Andreas Spanias, “On the Design of Deep Priors for Unsupervised Audio Restoration,” in *Proc. Interspeech*, 2021, pp. 2167–2171.
- [2] Pavel Závíška, Pavel Rajmic, Alexey Ozerov, and Lucas Rencker, “A survey and an extensive evaluation of popular audio declipping methods,” *IEEE Journal of Selected Topics in Signal Proc.*, vol. 15, no. 1, pp. 5–24, 2021.
- [3] Johannes Imort, Giorgio Fabbro, Marco A. Martínez Ramírez, Stefan Uhlich, Yuichiro Koyama, and Yuki Mitsufuji, “Distortion Audio Effects: Learning How to Recover the Clean Signal,” in *Proc. ISMIR*, 2022.
- [4] Volodymyr Kuleshov, S. Zayd Enam, and Stefano Ermon, “Audio super resolution using neural networks,” *ArXiv*, vol. abs/1708.00853, 2017.
- [5] Eloi Moliner and Vesa Välimäki, “BEHM-GAN: bandwidth extension of historical music using generative adversarial networks,” *IEEE ACM Trans. Audio Speech Lang. Process.*, vol. 31, pp. 943–956, 2023.
- [6] Chenshuang Zhang, Chaoning Zhang, Sheng Zheng, Mengchun Zhang, Maryam Qamar, Sung-Ho Bae, and In So Kweon, “A survey on audio diffusion models: Text to speech synthesis and enhancement in generative AI,” *CoRR*, vol. abs/2303.13336, 2023.
- [7] Eloi Moliner, Jaakko Lehtinen, and Vesa Välimäki, “Solving audio inverse problems with a diffusion model,” in *IEEE Int. Conf. Ac. Speech Signal Process. (ICASSP)*, 2023, pp. 1–5.
- [8] Koichi Saito, Naoki Murata, Toshimitsu Uesaka, Chieh-Hsin Lai, Yuhta Takida, Takao Fukui, and Yuki Mitsufuji, “Unsupervised vocal dereverberation with diffusion-based generative models,” in *IEEE Int. Conf. Ac. Speech Signal Process. (ICASSP)*, 2023, pp. 1–5.
- [9] Arnon Turetzky, Tzvi Michelson, Yossi Adi, and Shmuel Peleg, “Deep Audio Waveform Prior,” in *Proc. Interspeech*, 2022, pp. 2938–2942.
- [10] Naoki Murata, Koichi Saito, Chieh-Hsin Lai, Yuhta Takida, Toshimitsu Uesaka, Yuki Mitsufuji, and Stefano Ermon, “GibbsDDRM: A partially collapsed gibbs sampler for solving blind inverse problems with denoising diffusion restoration,” in *ICML*, 2023.
- [11] Hyungjin Chung, Jeongsol Kim, Michael T. McCann, Marc Louis Klasky, and Jong Chul Ye, “Diffusion posterior sampling for general noisy inverse problems,” *CoRR*, vol. abs/2209.14687, 2022.
- [12] Jonathan Ho, Tim Salimans, Alexey Gritsenko, William Chan, Mohammad Norouzi, and David J Fleet, “Video diffusion models,” in *Advances in Neural Inf. Proc. Systems*, 2022, vol. 35, pp. 8633–8646.
- [13] Jooyoung Choi, Sungwon Kim, Yonghyun Jeong, Youngjune Gwon, and Sungroh Yoon, “Ilvr: Conditioning method for denoising diffusion probabilistic models,” in *IEEE/CVF International Conf. on Computer Vision (ICCV)*, 2021, pp. 14347–14356.
- [14] Jiaming Song, Arash Vahdat, Morteza Mardani, and Jan Kautz, “Pseudoinverse-guided diffusion models for inverse problems,” in *ICLR*, 2023.
- [15] Andreas Lugmayr, Martin Danelljan, Andrés Romero, Fisher Yu, Radu Timofte, and Luc Van Gool, “Repaint: Inpainting using denoising diffusion probabilistic models,” in *IEEE/CVF Conf. on Comp. Vision and Pattern Rec.* 2022, pp. 11451–11461, IEEE.
- [16] Tuomas Virtanen, Annamaria Mesáros, and Matti Ryyänen, “Combining pitch-based inference and non-negative spectrogram factorization in separating vocals from polyphonic music,” in *Proc. Interspeech*, 2008.
- [17] Jiwen Yu, Yinhuai Wang, Chen Zhao, Bernard Ghanem, and Jian Zhang, “Freedom: Training-free energy-guided conditional diffusion model,” *CoRR*, vol. abs/2303.09833, 2023.
- [18] Moshe Mandel, Or Tal, and Yossi Adi, “Aero: Audio super resolution in the spectral domain,” in *IEEE Int. Conf. Ac. Speech Signal Process. (ICASSP)*, 2023, pp. 1–5.
- [19] Bahjat Kawar, Michael Elad, Stefano Ermon, and Jiaming Song, “Denoising diffusion restoration models,” in *NeurIPS*, 2022.
- [20] Jascha Sohl-Dickstein, Eric Weiss, Niru Maheswaranathan, and Surya Ganguli, “Deep unsupervised learning using nonequilibrium thermodynamics,” in *ICML*. PMLR, 2015, pp. 2256–2265.
- [21] Jonathan Ho, Ajay Jain, and Pieter Abbeel, “Denoising diffusion probabilistic models,” in *NeurIPS*, 2020.
- [22] Tero Karras, Miika Aittala, Timo Aila, and Samuli Laine, “Elucidating the design space of diffusion-based generative models,” in *NeurIPS*, 2022.
- [23] Aapo Hyvärinen, “Estimation of non-normalized statistical models by score matching,” *Journal of Machine Learning Research*, vol. 6, no. 24, pp. 695–709, 2005.
- [24] Yang Song, Jascha Sohl-Dickstein, Diederik P Kingma, Abhishek Kumar, Stefano Ermon, and Ben Poole, “Score-based generative modeling through stochastic differential equations,” in *International Conference on Learning Representations*, 2021.
- [25] Bidisha Sharma, Xiaoxue Gao, Karthika Vijayan, Xiaohai Tian, and Haizhou Li, “NHSS: A speech and singing parallel database,” *Speech Commun.*, vol. 133, pp. 9–22, 2021.
- [26] Zhiyan Duan, Haotian Fang, Bo Li, Khe Chai Sim, and Ye Wang, “The NUS sung and spoken lyrics corpus: A quantitative comparison of singing and speech,” in *APSIPA*, 2013, pp. 1–9.
- [27] Zafar Rafii, Antoine Liutkus, Fabian-Robert Stöter, Stylianos Ioannis Mimilakis, and Rachel Bittner, “The MUSDB18 corpus for music separation,” Dec. 2017.
- [28] Gino Angelo Velasco, Nicki Holighaus, Monika Dorerfler, and Thomas Grill, “Constructing an invertible constant-q transform with nonstationary gabor frames,” in *Proc. DAFx*, 09 2011.
- [29] Kevin Kilgour, Mauricio Zuluaga, Dominik Roblek, and Matthew Sharifi, “Fréchet audio distance: A reference-free metric for evaluating music enhancement algorithms,” in *Proc. Interspeech*. 2019, pp. 2350–2354, ISCA.
- [30] Jonathan Le Roux, Scott Wisdom, Hakan Erdogan, and John R. Hershey, “Sdr – half-baked or well done?,” in *IEEE Int. Conf. Ac. Speech Signal Process. (ICASSP)*, 2019, pp. 626–630.
- [31] International Telecommunication Union, “Method for the subjective assessment of intermediate quality level of audio systems,” ITU-R Recommendation ITU-R BS.1534-3, 2015.